ROCKET-2: Steering Visuomotor Policy via Cross-View Goal Alignment

Shaofei Cai¹, Zhancun Mu¹, Anji Liu² and Yitao Liang ⊠¹

We aim to develop a goal specification method that is semantically clear, spatially sensitive, domain-agnostic, and intuitive for human users to guide agent interactions in 3D environments. Specifically, we propose a novel cross-view goal alignment framework that allows users to specify target objects using segmentation masks from their camera views rather than the agent's observations. We highlight that behavior cloning alone fails to align the agent's behavior with human intent when the human and agent camera views differ significantly. To address this, we introduce two auxiliary objectives: cross-view consistency loss and target visibility loss, which explicitly enhance the agent's spatial reasoning ability. According to this, we develop ROCKET-2, a state-of-the-art agent trained in Minecraft, achieving an improvement in the efficiency of inference $3 \times$ to $6 \times$ compared to ROCKET-1. We show that ROCKET-2 can directly interpret goals from human camera views, enabling better human-agent interaction. Remarkably, ROCKET-2 demonstrates zero-shot generalization capabilities: despite being trained exclusively on the Minecraft dataset, it can adapt and generalize to other 3D environments like Doom, DMLab, and Unreal through a simple action space mapping. The project page is available at https://craftjarvis.github.io/ROCKET-2/.

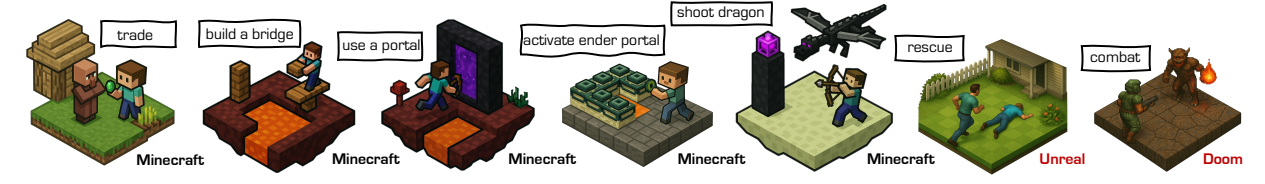


Figure 1 | Powered by cross-view goal specification, we are the first to show that AI agents can complete complex tasks such as *building a bridge* and *damaging the dragon* in Minecraft. In addition, it demonstrates an impressive zero-shot generalization to other 3D games.

1. Introduction

Learning an agent to achieve desired goals is a long-standing challenge in the field of embodied intelligence, with significant implications for the development of robots (Brohan et al., 2022, 2023; Jang et al., 2022) and virtual players (Wang et al., 2023b,c,d). A key challenge is to find goal representations that are (i) flexible for human users to specify and (ii) expressive and precise to capture as many tasks as possible. Most current approaches address only one of these aspects. For example, traditional works (Brohan et al., 2022; Driess et al., 2023; Lynch et al., 2023) focus on training agents to follow language instructions. As pointed out in Cai et al. (2025a); Sundaresan et al., while language is intuitive, it relies on numerous prepositions to express spatial relationships, which can be vague and inefficient. Furthermore, language also suffers from the generalization problem of novel visual concepts (Cai et al., 2023). Realizing these limitations, some works attempted to introduce visual modalities into goal representations. For example, Sundaresan et al. employs hand-drawn target layouts in robot manipulation environments to represent human intent; Gu et al. (2023) uses end-effector trajectory sketches for fine-grained control of robot arms; and ROCKET-1 (Cai et al., 2025a) specifies the objects to interact with by applying segmentation masks to the agent's perception. These methods greatly improved the expressiveness of spatial relationships and generalization across tasks. However, both trajectory sketches and object segmentation are closely tied to the agent's current observation, causing issues in partially ob-

¹Peking University, ²University of California, Los Angeles, All authors are affiliated with Team CraftJarvis

servable 3D worlds. These include: (i) goals need to be generated in real-time as the agent's camera view changes; (ii) goals cannot be specified when the target is occluded.

To strike a balance between expressiveness and flexibility, we propose an innovative and userfriendly cross-view goal specification method. It allows human users to specify the target object using segmentation masks from their own camera view, rather than the agent's camera view. The agent is then trained to align with human intent and take actions based on its own observations via imitation learning. Decoupling the goal specification from the camera view of the agent will significantly enhance the efficiency of human-agent interaction. However, the partial observability of open worlds makes aligning goals across camera views challenging. This involves handling occlusion, geometric deformation, and the distinction of objects of similar look. In Figure 1, we show an agent in the left corner and a human player standing on a farmland. The human intends to command the agent to hunt a sheep near the house, even though the agent cannot initially observe the target sheep. To achieve this, the agent must establish spatial relationships using shared visual landmarks between the human's camera view and its own. We find that relying solely on a behavior cloning loss is insufficient.

To address these challenges, we highlight an important property of behavior datasets (Cai et al., 2025a): The target object remains consistent across camera views in an interaction trajectory. Motivated by this, we propose two auxiliary objective functions: cross-view consistency loss and target visibility loss, to explicitly enhance the agent's ability to align goals across camera views. Specifically, cross-view consistency loss requires the agent to accurately predict the target object's centroid point w.r.t. its camera view, while target visibility loss helps the agent determine whether the target object is occluded. By combining these auxiliary losses with behavior cloning loss, we develop ROCKET-2, a state-ofthe-art agent in Minecraft. Our experiments show that ROCKET-2 can autonomously track the target object as the camera changes, eliminating the need for SAM's (Ravi et al., 2024) real-time se-

mantic segmentation, speeding up inference 3× to 6× compared to ROCKET-1. We observe that ROCKET-2 can interpret intentions from a human's camera view and make decisions to achieve expected goals in the 3D world. Notably, by simply mapping Minecraft's action space to that of other 3D environments, such as Doom (Kempka et al., 2016), DMLab (Beattie et al., 2016), and Unreal Engine (Zhong et al., 2024), we are surprised to find that ROCKET-2 could successfully perform basic navigation and object interaction tasks in a zero-shot generalization manner. This demonstrates that our proposed crossview alignment scheme is domain-agnostic and holds large potential for further scaling across a wider range of environments.

Our contributions are threefold: (1) We introduce a user-friendly interface that allows humans to specify goals using instance-segmentation from humans' camera view. (2) By introducing *crossview consistency loss* and *target visibility loss*, we train ROCKET-2, an agent that autonomously tracks targets, eliminating the need for real-time goal segmentation and significantly speeding up inference. (3) We demonstrate that ROCKET-2, trained solely on Minecraft data, can zero-shot generalize to other 3D environments, which opens new avenues for discovering universal decision representations in 3D environments.

2. Related Works

Partial Observability. We address policy learning in partially observable 3D environments (Cai et al., 2024; Savva et al., 2019), where the agent perceives only egocentric views and must actively explore to locate key objects (Pearce and Zhu, 2022). Some methods leverage 3D point clouds for global context (Huang et al., 2023; Jiang et al., 2024), but such data is often unavailable. More commonly, memory-based architectures are used to aggregate past observations: RNNs help avoid redundant exploration (Gadre et al., 2022; Zhao et al., 2023), and TransformerXL enables longhorizon planning in Minecraft (Baker et al., 2022; Guss et al., 2019). To mitigate partial observability, some works (Krantz et al., 2022, 2023) use instance images to specify goals, but these require

unoccluded, centered views where the object occupies most of the image—constraints that limit their applicability. Instead, we require the policy to align object references across egocentric views, enabling robust target tracking under camera motion. While cross-view alignment has been explored in computer vision for BEV segmentation (Borse et al., 2023) and re-identification (Xu et al., 2019), we are the first to apply it to openworld policy learning.

Goal-Conditioned Imitation Learning. GCIL optimizes conditional policies via behavior cloning (Pomerleau, 1988), using goal representations such as language (Brohan et al., 2022, 2023; Lynch et al., 2023), images (Lifshitz et al., 2023; Majumdar et al., 2022; Sundaresan et al.), videos (Cai et al., 2023, 2025b), or trajectory sketches (Gu et al., 2023; Wang et al., 2023a). Compared to standard imitation learning, GCIL provides clearer targets, simplifies behavior modeling, and improves policy controllability. Language goals are commonly used (Driess et al., 2023; Padalkar et al., 2023; Wang et al., 2023d) but often fail to convey spatial details (Cai et al., 2025a; Gu et al., 2023). Image goals (Majumdar et al., 2022; Wang et al., 2023a) better ground spatial intent but are sensitive to lighting, textures, and other irrelevant features. Sketches (Sundaresan et al.) reduce visual sensitivity but are difficult to generate. Trajectory sketches (Gu et al., 2023) improve control and generalization, but assume full observability, limiting their use in 3D worlds. We instead propose aligning goal-relevant objects across views, enabling spatially grounded yet robust goal conditioning in partially observable environments.

3. Method

In this section, we first introduce the problem of cross-view segmentation-conditioned policy, discussing it from the perspective of imitation learning. Next, we describe the process of generating cross-view trajectories annotated with semantic segmentation. We then present two auxiliary objectives designed to enhance cross-view object alignment in 3D scenes: the *cross-view consistency loss* and the *target visibility loss*. Finally, we detail the architecture of ROCKET-2 and outline the

overall optimization objectives.

Problem Statement. Our goal is to learn a goal-conditioned visuomotor policy, which allows humans to specify goal objects for interaction using semantic segmentation across camera views. Formally, we aim to learn a policy $\pi_{\text{cross}}(a_t|o_{1:t}, \{o_g, m_g\}, c_g)$, where a_t represents the action at time t, c_g denotes the interaction event, such as break item, kill entity, and approach. In the Minecraft environment, an action corresponds to raw mouse and keyboard inputs. $o_t \in \mathbb{R}^{H \times W \times 3}$ denotes the environment observation at time t, and $o_g \in \mathbb{R}^{H \times W \times 3}$ represents an observation of the local environment from a specific camera view. Generally, o_g and o_t have some visual content overlap. $m_g \in \{0,1\}^{H \times W \times 1}$ is a segmentation mask for og, highlighting the target object within the camera view o_g . During inference, users select a view o_g containing the desired object from historical observations returned by the environment and generates its corresponding semantic segmentation m_g . To train such visuomotor policy, we assume access to a dataset $\mathcal{D}_{\text{cross}} = \{c^n, (o_t^n, a_t^n, m_t^n)_{t=1}^{L(n)}\}_{n=1}^N \text{ consisting of } N$ successful demonstration episodes, L(n) is the length of episode n. Within each episode, if m_t is non-empty, all (o_t, m_t) pairs indicate the same object. Consequently, we can arbitrarily pick one observation frame as the goal view condition for the entire trajectory.

Cross-View Dataset Generation. Without loss of generality, we use the Minecraft world as an example to illustrate the data generation process. Manually collecting datasets that meet the requirements is highly expensive. Thus, we employ the backward trajectory relabeling technique proposed in Cai et al. (2025a) to automate the annotation of the OpenAI Contractor Dataset (Baker et al., 2022), which consists of free-play trajectories from human players: $\mathcal{D}_{\text{raw}} = \{(o_t^n, a_t^n)_{t=1}^{L(n)}\}_{n=1}^N$. Specifically, for any given episode n, we first detect all frames o_i^n where interaction events occur, identify the interaction type c_i^n , and localize the interacted object near frame j using bounding boxes and point-based prompts. The SAM-2 (Ravi et al., 2024) model is then employed to generate the segmentation mask m_i^n for the object. Starting from frame i, we traverse the trajectory

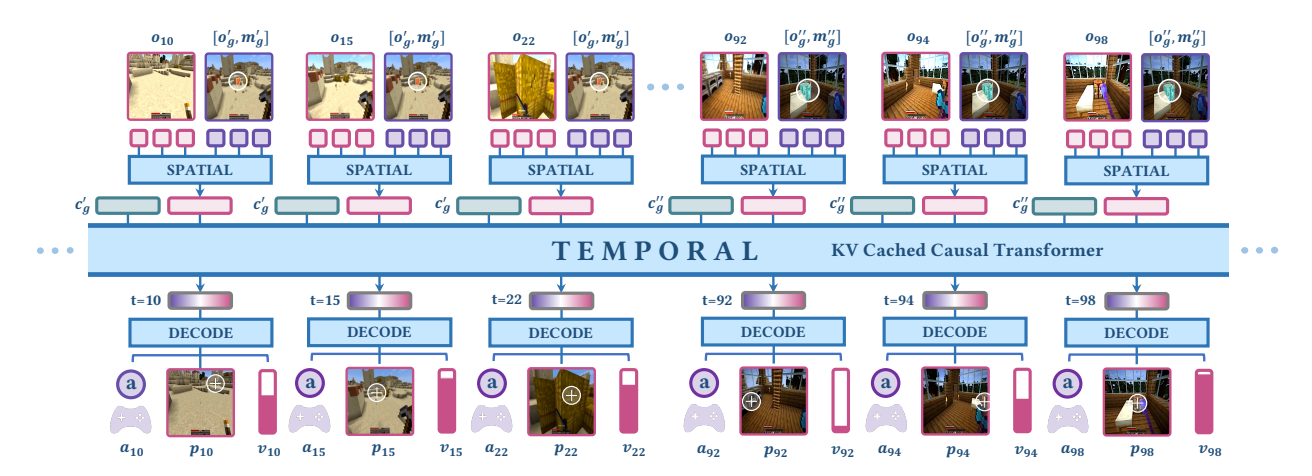


Figure 2 | **Overview of our approach.** We address the challenge of steering visuomotor policy via cross-view goal alignment. Our method allows humans to specify goals from their camera view while the agent acts based on its own observations.

backward and use the SAM-2 model to continuously generate segmentation masks for the object in real-time until either a new interaction event is encountered or a maximum tracking length is reached. Let i denote the end frame. The resulting trajectory clip is then added to the training dataset: $\mathcal{D}_{\text{cross}} \leftarrow \mathcal{D}_{\text{cross}} \cup \{c_j, (o_t^n, a_t^n, m_t^n)_{t=i}^j\}$. This ensures that every extracted clip is associated with a consistent interaction intent. The generated data encompasses the fundamental interaction types in Minecraft, including use, break, approach, craft, and kill entity. Among these, approach is a unique event, identified by detecting trajectory clips where the displacement exceeds a specified threshold. The object located at the center of the clip's final frame is designated as the goal of the approach event.

Cross-View Consistency Loss. Accurately interpreting the cross-view goal requires the policy to possess cross-view visual object alignment ability in 3D scenes. To achieve this, the model must fully exploit visual cues from different camera views, such as scene layout and landmark buildings, while being robust to challenges like occlusion, shape variations, and changes in distance. We observe that relying solely on behavior cloning loss (Pomerleau, 1988) is insufficient. Therefore, we propose a *cross-view consistency loss*. Since the segmentation across different camera views corresponds to the same object, we train the model to condition on the segmentation from one camera view to generate the segmen-

tation for another camera view, thereby directly enhancing the model's 3D spatial perception. To reduce computational complexity, we opt to predict the centroid of the segmentation mask instead of the complete mask, formally expressed as: $\pi_{cross}(p_t \mid o_{1:t}, \{o_g, m_g\}, c_g)$, where

$$p_t = \frac{\sum_{i=1}^{H} \sum_{j=1}^{W} (i, j) \cdot m_t(i, j)}{\sum_{i=1}^{H} \sum_{j=1}^{W} m_t(i, j)}.$$
 (1)

It is worth noting that incorporating the historical observations $o_{1:t-1}$ as input is essential, especially when there is limited shared visual content between o_t and o_g . This historical sequence acts as a smooth bridge to facilitate alignment. Since the goal object represented by the mask corresponds to the target of the policy's interaction, this auxiliary task aligns the policy's actions with its visual focus, effectively improving task performance.

Target Visibility Loss. Due to the partial observability in 3D environments, it is common for target objects in interaction trajectories to disappear from the field of view and reappear later. During such intervals, the segmentation mask for the missing object is empty. To leverage this information, we propose training the model to predict whether the target object is currently visible, formulated as: $\pi_{cross}(v_t \mid o_{1:t}, \{o_g, m_g\})$, where v_t is a binary indicator for empty segmentation masks. On the one hand, accurately predicting object visibility helps the policy better match the target object, avoiding a simple appearance similarity

measurement between two frames. On the other hand, visibility information guides the policy to make reasonable decisions, such as confidently approaching the goal when it is visible or actively adjusting its camera to explore when the target is absent.

ROCKET-2 Architecture. Let a training trajectory n be denoted as $(c_g, \{o_t, m_t\}_{t=1}^{L(n)})$. A cross view index g is sampled from $\{i|i \in [1, L(n)], m_i \neq \phi\}$. We resize all visual observations and their segmentation masks to 224 × 224. For encoding the visual observation o_t , we utilize a DINOpretrained (Caron et al., 2021) 3-channel ViT-B/16 (Dosovitskiy et al., 2020) (16 is the patch size), which outputs a token sequence of length 196, denoted as $\{\hat{o}_t^i\}_{i=1}^{196}$. Inspired by Zhong et al. (2025), we encode the segmentation mask m_t using a 1-input-channel ViT-tiny/16, yielding $\{\hat{m}_t^i\}_{i=1}^{196}$. The ViT-base/16 encoder is frozen during training for efficiency, while the ViT-tiny/16 is trainable. To ensure spatial alignment, we fuse the cross-view condition (o_g, m_g) by concatenating the feature channels:

$$h_g^i = \text{FFN}(\text{concat}([\hat{o}_g^i \parallel \hat{m}_g^i])).$$
 (2)

Given the ability of self-attention mechanisms to capture spatial details across views, we concatenate the token sequences from two views into a sequence of length 392. A non-causal Transformer encoder module is applied (Vaswani et al., 2017) for spatial fusion, obtaining a frame-level representation x_t :

$$x_t \leftarrow \text{SpatialFusion}(\{\hat{o}_t^i\}_{i=1}^{196}, \{h_g^i\}_{i=1}^{196}).$$
 (3)

Then, we leverage a causal TransformerXL (Dai et al., 2019) architecture to capture temporal information among frames:

$$f_t \leftarrow \text{TransformerXL}(\{x_i\}_{i=1}^t, c_g).$$
 (4)

Finally, a light network maps f_t to predict action \hat{a}_t , centroid \hat{p}_t , and visibility \hat{v}_t . The loss function for episode n follows:

$$\mathcal{L}(n) = \sum_{t=1}^{L(n)} -a_t^n \log \hat{a}_t^n - p_t^n \log \hat{p}_t^n - v_t^n \log \hat{v}_t^n.$$
 (5)







Figure 3 | The Evaluation Metric is Spatial-Sensitive. \checkmark and \times indicate the correct and incorrect objects for interaction, respectively. None of the task is trained.

4. Experiments

We aim to address the following questions: (1) How does ROCKET-2 perform in terms of both accuracy and efficiency during inference? (2) Can ROCKET-2 follow the intent of a human from a cross-camera view in Minecraft? (3) Can ROCKET-2 adapt and generalize to other 3D environments? (4) How important are landmarks in cross-view goal alignment for ROCKET-2? (5) Can ROCKET-2 interpret goal views from cross-episode scenarios? (6) Which modules contribute effectively to training ROCKET-2?

4.1. Experimental Setup

We include all the details, such as hyperparameters, benchmarks, case studies and extensive experiments, in the Appendix.

Environment and Benchmark. We use Minecraft v1.16.5 (Cai et al., 2024; Guss et al., 2019) as the testing environment, which accepts mouse and keyboard inputs and returns a 640 × 360 RGB image per step. Following Cai et al. (2025a), we employ the Minecraft Interaction Benchmark to evaluate the agent's interaction capabilities. This benchmark includes six categories and a total of 12 tasks, covering all basic Minecraft interaction types: Hunt, Mine, Interact, Navigate, Tool, and *Place.* As this benchmark emphasizes object interaction and spatial localization, its evaluation criteria are more stringent than those in Lifshitz et al. (2023) and Cai et al. (2023). We present three examples in Figure 3, more can be found in appendix. In the "hunt the sheep in the right fence" task, success requires the agent to kill the sheep within the right fence, while killing sheep in the left fence results in failure.

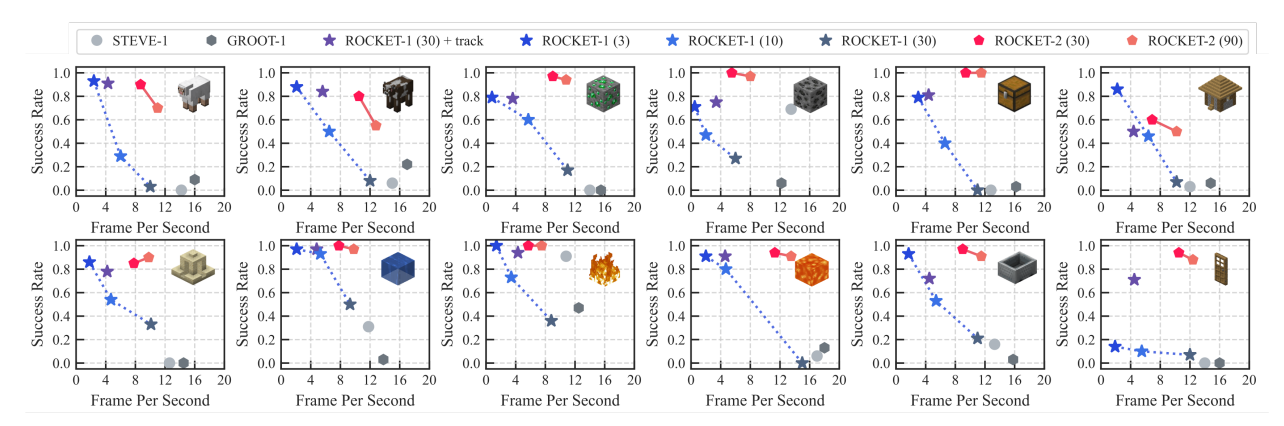


Figure 4 | Minecraft Interaction Benchmark Results. Our ROCKET-2 achieves $3 \times$ to $6 \times$ faster inference, matching or surpassing ROCKET-1's peak performance in most tasks. Numbers in parentheses indicate Molmo invocation interval (steps); larger values mean higher FPS. + track denotes real-time SAM-2 tracking between Molmo calls.

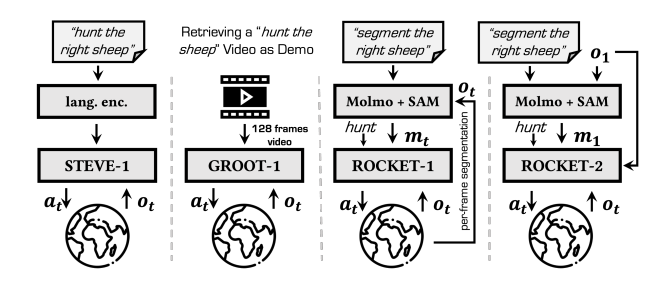


Figure 5 | Inference Pipelines on Minecraft Interaction Benchmark. GROOT-1 requires retreving a short video as its condition. ROCKET-1's segmentation is coupled with the agent's real-time observations, whereas ROCKET-2's segmentation is solely tied to the third-person view.

Baselines. We compare our ROCKET-2 with the following instruction-following baselines: (1) STEVE-1 (Lifshitz et al., 2023): A textconditioned agent fine-tuned from VPT (Baker et al., 2022), capable of solving various shorthorizon tasks. (2) GROOT-1 (Cai et al., 2023): A video-conditioned policy designed for openended tasks, implemented with a VAE network. (3) ROCKET-1 (Cai et al., 2025a): A maskconditioned policy capable of mastering 12 interaction tasks. Taking the hunt right sheep task as an example, we present the inference pipelines in Figure 5, where Molmo (Deitke et al., 2024) and SAM (Ravi et al., 2024) are combined to perform text-based instance segmentation. Given that ROCKET-2 relies on a third-person viewpoint for goal specification, in the Minecraft Interaction Benchmark, we set its third-person view to the observation acquired by the agent at the initial step. This view is then largely maintained, undergoing resets only at fixed periods (e.g., every 90 steps). This setup ensures that ROCKET-2 requires no additional privileged information.

4.2. Performance-Efficiency Analysis

Figure 4 presents our Minecraft Interaction Benchmark results, showcasing various agent configurations and their performance. Specifically, ROCKET-1 (10) performs object segmentation with Molmo + SAM every 10 steps, providing no masks for the intermediate 9 steps; its "+ track" variant leverages SAM's more computationally efficient object tracking to causally generate masks for these frames. In contrast, ROCKET-2 utilizes cross-view segmentation, only requiring a single third-person view segmentation, with ROCKET-2 (90) resetting this view every 90 steps. Our initial observations highlight that STEVE-1 and GROOT-1 exhibit success rates below 20% across most tasks, primarily due to their instructions' limited spatial sensitivity. While ROCKET-1 achieves over 80% success with high-frequency Molmo (every 3 frames), it suffers from slow inference; lowering Molmo's frequency or enabling SAM tracking (though still expensive) significantly degrades its performance. Conversely, our ROCKET-2 agent, by decoupling goal specification from the agent's current view, autonomously tracks targets without frequent mask modifications, achieving comparable or superior performance to ROCKET-1



Figure 6 | Case Study of Human-Agent Interaction. We show how a human interacts with ROCKET-2, leveraging its spatial reasoning abilities. (Top Row) The human specifies a hay bale () that is not visible to ROCKET-2. By exploring the area around the visible landmark (house), ROCKET-2 successfully locates the goal. (Bottom Row) Human specifies a target tree in the presence of a tree distractor. ROCKET-2 accurately identifies the correct tree by reasoning about spatial relationships. The trajectories are visualized in BEV maps.

with a remarkable $3 \times$ to $6 \times$ inference speedup.

4.3. Intuitive Human-Agent Interaction

In Figure 6, we present two case studies illustrating ROCKET-2 interprets human intent under the cross-view goal specification interface. The first case (top row) involves a task requiring the agent to approach a hay bale () located behind a house (a). From the human view, both the house and the hay bale are visible, whereas ROCKET-2 initially observes only the house. A key challenge arises from the differing camera views: the human and ROCKET-2 perceive the scene from opposite sides of the house. To analyze the agent's behavior, we visualize both its camera views and its trajectories on a bird's-eye map. We observe that ROCKET-2 effectively infers the hay bale's potential location and successfully navigates toward it. This is reflected in the increasing target visibility score and the movement of the predicted point. Interestingly, the bird's-eye view reveals that ROCKET-2 approaches the target from both sides of the house, demonstrating diversity in route selection. The second case (bottom row) showcases ROCKET-2 's ability to distinguish between a distractor and the human-specified goal object, despite their visual similarity. It highlights that agent's spatial reasoning extends beyond object appearance.

4.4. Zero-Shot 3D Worlds Generalization

We demonstrate that by mapping the action space of Minecraft to unseen 3D games (refer to Table 1), ROCKET-2 achieves zero-shot generalization, despite being trained solely on the Minecraft dataset. We attribute this to two key factors: (1) the DINO-pretrained ViT backbone is frozen during training, preserving its general 3D view perception capability; and (2) the learned cross-view goal alignment skill is domain-agnostic. We evaluated ROCKET-2 in the ATEC 2025 AI and Robotics Challenge ¹, which is built in the Unreal Engine and assigns agents to locate injured people and transport them to stretchers. The benchmark provides both textual (a long text description) and visual cues (a third-person view) about the locations of the victims. Note that, ROCKET-2 takes in **solely visual cues** (Figure 7). As shown in Table 2, ROCKET-2 outperforms the strong baseline provided by the organizers, a Gemma-3 and YOLO-based two-tiered decision system using both textual and visual cues, by 12%, despite not being fine-tuned on the Unreal. Furthermore, the Unreal environment provides observations at a 640 × 480 resolution, a notable deviation from the 640×360 resolution of the training dataset. This robustly substantiates that cross-view goal alignment enables the acquisition of transferable

¹https://github.com/atecup/atec2025 software algorithm



Figure 7 | **Zero-Shot 3D Environment Generalization.** ROCKET-2 can find and transport the victim to the stretcher in the unseen **Unreal** Engine. We map the *left click/right click* actions of Minecraft to the *carry up/put down* actions of Unreal to interact with objects, respectively.

3D decision representations within one environment and their successful migration to another. Such capabilities underscore the significant feasibility of developing general-purpose multi-task agents for diverse 3D environments.

Table 1 | **Bridging the Minecraft Action Space and Other 3D Games.** "/" denotes the masked action.

Minecraft	DeepMind Lab	Doom	Unreal
forward = 1	a[3] = 1	discrete[2] = 1	velocity = +100
back = 1	a[3] = -1	discrete[3] = 1	velocity = -100
attack = 1	a[4] = 1	discrete[1] = 1	pick = 1
	• • •	• • •	• • •
yaw = x $pitch = x$	a[0] = 4.75x $a[1] = 2.78x$	continuous = x /	angular = x $viewport = x$

Table 2 | Results on ATEC 2025 Robotics Challenge.

Agent	ROCKET-2 (Zero-Shot)	YOLO-Gemma 3
Rank	1/57	20/57
Success Rate	38%	26%

4.5. Ablation Studies on Auxiliary Objectives

To evaluate the impact of auxiliary losses on model performance, we define three variants: (1) only behavior cloning loss, (2) + target visibility loss, and (3) the full version with + cross-view consistency loss. We conduct experiments on three tasks: Navigate to House in a Village(...), Mine Emerald(), and Interact with the Left Chest(). We find that the BC-only variant achieves an average success rate of only 65%, demonstrating that the action signal is insufficient for learning spatial alignment. Adding target visibility loss improves performance by 6%, while further incorporating cross-view consistency loss boosts the success rate to 94%. This proves that leveraging temporal consistency and introducing vision-based auxiliary losses can greatly enhance cross-view goal alignment and inference-time decision-making.

Table 3 | **Ablation Study on Auxiliary Objectives.** The final loss function for each row is the cumulative sum of all loss functions from the preceding ones.

Model Variants				Avg.
behavior cloning	0.52	0.78	0.65	0.65
+ target visibility	0.63	0.83	0.68	0.71
+ cross-view consistency	0.85	0.97	1.00	0.94

4.6. Landmarks Attention Visualization

Prominent non-goal objects, referred to as "land-marks", play a crucial role in assisting humans or agents in localizing goal objects within a scene. For instance, when multiple objects with similar appearances are present, spatial relationships between the goal and landmarks can aid in distinction. In this subsection, we aim to explore whether ROCKET-2 implicitly learns landmark alignment by visualizing the attention weights of its spatial transformer.

Specifically, we prepare a current view observation and a third view with goal segmentation. Before being fed into the spatial transformer, both views are encoded into $14 \times 14 = 196$ tokens: $\{\hat{o}_t^i\}_{i=1}^{196}$ and $\{h_g^i\}_{i=1}^{196}$ (notations are consistent with Sec. 3). We inspect the softmax-normalized attention map of the first self-attention layer in the spatial transformer, denoted as $\{a_{i,j}\}_{i,j=1}^{392}$, where $a_{i,197:392}$ represents the attention map generated by using patch i from the current view as the query and all patches from the third view as keys and values. This map is overlaid on the third view (goal view) to reflect its responsiveness to patch i in the current view. Since landmarks may span multiple patches, we aggregate the response maps of different patches to form the final attention map $\{m_i\}_{i=1}^{196}$: $m_i = \frac{1}{|L|} \sum_{x \in L} a_{x,i+196}$, where L denotes the set of patches in the current view representing a specific landmark. Notably, the

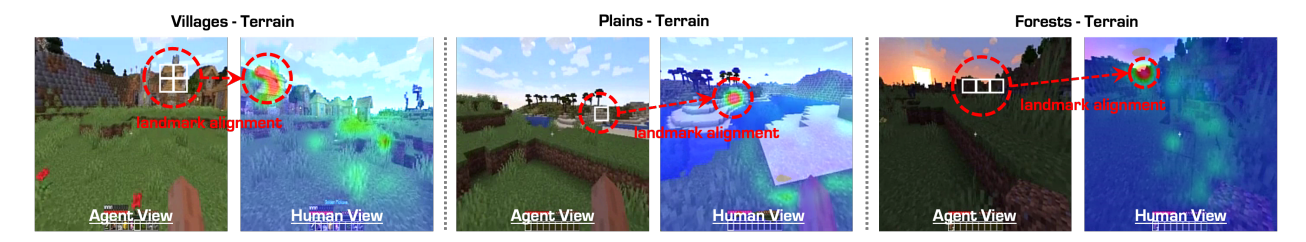


Figure 8 | **Visualization Analysis of Landmarks' Alignment.** The vision patches (identified by white grid) represent a chosen background landmark in the agent's current view (instead of the goal object). We generate an attention map with the **spatial fusion transformer** using these patches as queries and the human view patches as keys and values. We find that ROCKET-2 well aligns selected landmarks across views.



Figure 9 | **Cross-Episode Generalization.** The goal view does not exist within the agent's world but originates from a different episode. ROCKET-2 attempts to infer the semantic intent underlying the goal specification (building a bridge and approaching a house).

selected landmarks do not overlap with the goal segmentation. As shown in Figure 8, we present three sets of data covering *villages*, *plains*, and *forest* terrains. In the left plot, the white grid indicates the selected landmark patches, while the right plot shows the human-view attention response to the chosen landmarks. Our findings reveal that ROCKET-2 effectively matches crossview consistency even under significant geometric deformations and distance variations. Surprisingly, in the last data point, even subtle forest depressions are accurately matched.

4.7. Cross-Episode Cross-View Goal Alignment

We observe that ROCKET-2 exhibits crossepisode generalization capabilities. As shown in Figure 9, the selected goal views come from different episodes, each generated with a unique world seed. In the top-row example, the goal view is from a "bridge-building" episode set in the savanna biome, where the player is placing a dirt block to build the bridge. After feeding forward the goal view, we place ROCKET-2 in a forest biome and observe its behavior. We find that it first exhibits pillar-jumping behavior, and after placing many blocks, it begins to build the bridge horizontally. Although it ultimately failed to build the perfect bridge, the emergent behavior still indicates that ROCKET-2 attempts to understand the underlying semantic information when there is no landmark match across views. In the bottom row, the goal view is taken from a Minecraft creative mode, observing a house from the sky— a view never seen during training. We find that ROCKET-2 explores its environment and successfully identifies a visually similar house. This demonstrates ROCKET-2 's robustness to a variety of goal views.

5. Conclusion

We propose a cross-view goal specification method to improve human-agent interaction in embodied worlds. To address misalignment between agent and human views, we introduce cross-view consistency and visibility losses. Our agent sets a new benchmark on the *Minecraft Interaction Benchmark*, achieving $3\times-6\times$ higher efficiency. Visualizations support the effectiveness of our method. Our zero-shot generalization results underscore the promise of cross-view goal alignment as a core for building general-purpose decision-making agents in 3D worlds.

Acknoledgements

This work was supported by the National Science and Technology Major Project #2022ZD0114902. We sincerely appreciate their generous support, which enabled us to conduct this research.

References

Marcin Andrychowicz, Dwight Crow, Alex Ray, Jonas Schneider, Rachel Fong, Peter Welinder, Bob McGrew, Joshua Tobin, P. Abbeel, and Wojciech Zaremba. Hindsight experience replay. *ArXiv*, abs/1707.01495, 2017. URL https://api.semanticscholar.org/CorpusID:3532908. 17

Bowen Baker, Ilge Akkaya, Peter Zhokhov, Joost Huizinga, Jie Tang, Adrien Ecoffet, Brandon Houghton, Raul Sampedro, and Jeff Clune. Video pretraining (vpt): Learning to act by watching unlabeled online videos. *ArXiv*, abs/2206.11795, 2022. URL https://api.semanticscholar.org/CorpusID:249953673. 2, 3, 6, 14, 16

Charles Beattie, Joel Z. Leibo, Denis Teplyashin, Tom Ward, Marcus Wainwright, Heinrich Küttler, Andrew Lefrancq, Simon Green, Víctor Valdés, Amir Sadik, Julian Schrittwieser, Keith Anderson, Sarah York, Max Cant, Adam Cain, Adrian Bolton, Stephen Gaffney, Helen King, Demis Hassabis, Shane Legg, and Stig Petersen. Deepmind lab, 2016. URL https://arxiv.org/abs/1612.03801. 2, 14, 16, 18

Shubhankar Borse, Marvin Klingner, Varun Ravi Kumar, Hong Cai, Abdulaziz Almuzairee, Senthil Yogamani, and Fatih Porikli. X-align: Cross-modal cross-view alignment for bird's-eye-view segmentation. In *Proceedings of the IEEE/CVF Winter Conference on Applications of Computer Vision*, pages 3287–3297, 2023. 3

Anthony Brohan, Noah Brown, Justice Carbajal, Yevgen Chebotar, Joseph Dabis, Chelsea Finn, Keerthana Gopalakrishnan, Karol Hausman, Alexander Herzog, Jasmine Hsu, Julian Ibarz, Brian Ichter, Alex Irpan, Tomas Jackson, Sally Jesmonth, Nikhil J. Joshi, Ryan C. Julian, Dmitry Kalashnikov, Yuheng Kuang, Isabel Leal, Kuang-Huei Lee, Sergey Levine, Yao Lu, Utsav Malla, Deeksha Manjunath, Igor Mordatch, Ofir Nachum, Carolina Parada, Jodilyn Peralta, Emily Perez, Karl Pertsch, Jornell Quiambao, Kanishka Rao, Michael S. Ryoo, Grecia Salazar, Pannag R. Sanketi, Kevin Sayed, Jaspiar Singh, Sumedh Anand Sontakke, Austin Stone, Clayton Tan, Huong Tran, Vincent Vanhoucke, Steve Vega, Quan Ho Vuong, F. Xia, Ted Xiao, Peng Xu, Sichun Xu, Tianhe Yu, and Brianna Zitkovich. Rt-1: Robotics transformer for realworld control at scale. *ArXiv*, abs/2212.06817, 2022. URL https://api.semanticscholar.org/CorpusID:254591260. 1, 3

Anthony Brohan, Noah Brown, Justice Carbajal, Yevgen Chebotar, Xi Chen, Krzysztof Choromanski, Tianli Ding, Danny Driess, Avinava Dubey, Chelsea Finn, et al. Rt-2: Visionlanguage-action models transfer web knowledge to robotic control. *arXiv preprint arXiv:2307.15818*, 2023. 1, 3

Shaofei Cai, Bowei Zhang, Zihao Wang, Xiaojian Ma, Anji Liu, and Yitao Liang. Groot: Learning to follow instructions by watching gameplay videos. In *The Twelfth International Conference on Learning Representations*, 2023. 1, 3, 5, 6

Shaofei Cai, Zhancun Mu, Kaichen He, Bowei Zhang, Xinyue Zheng, Anji Liu, and Yitao Liang. Minestudio: A streamlined package for minecraft ai agent development. 2024. URL https://api.semanticscholar.org/CorpusID:274992448. 2, 5, 14, 16

Shaofei Cai, Zihao Wang, Kewei Lian, Zhancun Mu, Xiaojian Ma, Anji Liu, and Yitao Liang. Rocket-1: Mastering open-world interaction with visual-temporal context prompting. In *Proceedings of the Computer Vision and Pattern Recognition Conference (CVPR)*, pages 12122–12131, June 2025a. 1, 2, 3, 5, 6, 14, 17

Shaofei Cai, Bowei Zhang, Zihao Wang, Haowei Lin, Xiaojian Ma, Anji Liu, and Yitao Liang. GROOT-2: Weakly supervised multimodal instruction following agents. In *The Thirteenth International Conference on Learning Representations*, 2025b. URL https://openreview.net/forum?id=S9GyQUXzee. 3

- Mathilde Caron, Hugo Touvron, Ishan Misra, Hervé Jégou, Julien Mairal, Piotr Bojanowski, and Armand Joulin. Emerging properties in self-supervised vision transformers. In *Proceedings of the International Conference on Computer Vision (ICCV)*, 2021. 5
- Zihang Dai, Zhilin Yang, Yiming Yang, Jaime Carbonell, Quoc Le, and Ruslan Salakhutdinov. Transformer-xl: Attentive language models beyond a fixed-length context. In *Proceedings of the 57th Annual Meeting of the Association for Computational Linguistics*, Jan 2019. doi: 10.18653/v1/p19-1285. URL http://dx.doi.org/10.18653/v1/p19-1285. 5
- Matt Deitke, Christopher Clark, Sangho Lee, Rohun Tripathi, Yue Yang, Jae Sung Park, et al. Molmo and pixmo: Open weights and open data for state-of-the-art multimodal models, 2024. URL https://arxiv.org/abs/2409.17146.6
- Alexey Dosovitskiy, Lucas Beyer, Alexander Kolesnikov, Dirk Weissenborn, Xiaohua Zhai, Thomas Unterthiner, Mostafa Dehghani, Matthias Minderer, Georg Heigold, Sylvain Gelly, Jakob Uszkoreit, and Neil Houlsby. An image is worth 16x16 words: Transformers for image recognition at scale. *ArXiv*, abs/2010.11929, 2020. URL https://api.semanticscholar.org/CorpusID:225039882.
- Danny Driess, Fei Xia, Mehdi SM Sajjadi, Corey Lynch, Aakanksha Chowdhery, Brian Ichter, Ayzaan Wahid, Jonathan Tompson, Quan Vuong, Tianhe Yu, et al. Palm-e: An embodied multimodal language model. *arXiv preprint arXiv:2303.03378*, 2023. 1, 3
- Samir Yitzhak Gadre, Mitchell Wortsman, Gabriel Ilharco, Ludwig Schmidt, and Shuran Song. Clip on wheels: Zero-shot object navigation as object localization and exploration. *arXiv* preprint arXiv:2203.10421, 3(4):7, 2022. 2
- Jiayuan Gu, Sean Kirmani, Paul Wohlhart, Yao Lu, Montserrat Gonzalez Arenas, Kanishka Rao, Wenhao Yu, Chuyuan Fu, Keerthana Gopalakrishnan, Zhuo Xu, et al. Rt-trajectory: Robotic task generalization via hindsight trajectory

- sketches. *arXiv preprint arXiv:2311.01977*, 2023. 1, 3, 17
- William H. Guss, Brandon Houghton, Nicholay Topin, Phillip Wang, Cayden Codel, Manuela M. Veloso, and Ruslan Salakhutdinov. Minerl: A large-scale dataset of minecraft demonstrations. In International Joint Conference on Artificial Intelligence, 2019. URL https://api.semanticscholar.org/CorpusID:199000710. 2, 5
- Jiangyong Huang, Silong Yong, Xiaojian Ma, Xiongkun Linghu, Puhao Li, Yan Wang, Qing Li, Song-Chun Zhu, Baoxiong Jia, and Siyuan Huang. An embodied generalist agent in 3d world. arXiv preprint arXiv:2311.12871, 2023.
- Eric Jang, Alex Irpan, Mohi Khansari, Daniel Kappler, Frederik Ebert, Corey Lynch, Sergey Levine, and Chelsea Finn. Bc-z: Zeroshot task generalization with robotic imitation learning. *ArXiv*, abs/2202.02005, 2022. URL https://api.semanticscholar.org/CorpusID:237257594. 1
- Jiahao Jiang, Yuxiang Yang, Yingqi Deng, Chenlong Ma, and Jing Zhang. Bevnav: Robot autonomous navigation via spatial-temporal contrastive learning in bird's-eye view. *IEEE Robotics and Automation Letters*, 2024. 2
- Michał Kempka, Marek Wydmuch, Grzegorz Runc, Jakub Toczek, and Wojciech Jaśkowski. Vizdoom: A doom-based ai research platform for visual reinforcement learning. In 2016 IEEE Conference on Computational Intelligence and Games (CIG), page 1–8. IEEE Press, 2016. doi: 10.1109/CIG.2016.7860433. URL https://doi.org/10.1109/CIG.2016.7860433. 2, 14, 16, 18
- Jacob Krantz, Stefan Lee, Jitendra Malik, Dhruv Batra, and Devendra Singh Chaplot. Instance-specific image goal navigation: Training embodied agents to find object instances. *arXiv* preprint arXiv:2211.15876, 2022. 2
- Jacob Krantz, Theophile Gervet, Karmesh Yadav, Austin Wang, Chris Paxton, Roozbeh Mottaghi, Dhruv Batra, Jitendra Malik, Stefan Lee, and

- Devendra Singh Chaplot. Navigating to objects specified by images. In *Proceedings of the IEEE/CVF International Conference on Computer Vision*, pages 10916–10925, 2023. 2
- Shalev Lifshitz, Keiran Paster, Harris Chan, Jimmy Ba, and Sheila A. McIlraith. Steve-1: A generative model for text-to-behavior in minecraft. *ArXiv*, abs/2306.00937, 2023. URL https://api.semanticscholar.org/CorpusID:258999563. 3, 5, 6, 17
- Haowei Lin, Zihao Wang, Jianzhu Ma, and Yitao Liang. Mcu: A task-centric framework for openended agent evaluation in minecraft. *arXiv* preprint arXiv:2310.08367, 2023. 15
- Corey Lynch, Ayzaan Wahid, Jonathan Tompson, Tianli Ding, James Betker, Robert Baruch, Travis Armstrong, and Pete Florence. Interactive language: Talking to robots in real time. *IEEE Robotics and Automation Letters*, 2023. 1, 3, 17
- Arjun Majumdar, Gunjan Aggarwal, Bhavika Devnani, Judy Hoffman, and Dhruv Batra. Zson: Zero-shot object-goal navigation using multimodal goal embeddings. *ArXiv*, abs/2206.12403, 2022. URL https://api.semanticscholar.org/CorpusID:250048645.
- Abhishek Padalkar, Acorn Pooley, Ajinkya Jain, Alex Bewley, Alex Herzog, Alex Irpan, Alexander Khazatsky, Anant Rai, Anikait Singh, Anthony Brohan, et al. Open x-embodiment: Robotic learning datasets and rt-x models. arXiv preprint arXiv:2310.08864, 2023. 3, 17
- Tim Pearce and Jun Zhu. Counter-strike death-match with large-scale behavioural cloning. In *2022 IEEE Conference on Games (CoG)*, pages 104–111. IEEE, 2022. 2
- Dean A Pomerleau. Alvinn: An autonomous land vehicle in a neural network. *Advances in neural information processing systems*, 1, 1988. 3, 4
- Nikhila Ravi, Valentin Gabeur, Yuan-Ting Hu, Ronghang Hu, Chaitanya Ryali, Tengyu Ma, Haitham Khedr, Roman Rädle, Chloe Rolland, Laura Gustafson, Eric Mintun, Junting Pan,

- Kalyan Vasudev Alwala, Nicolas Carion, Chao-Yuan Wu, Ross Girshick, Piotr Dollár, and Christoph Feichtenhofer. Sam 2: Segment anything in images and videos. *arXiv preprint arXiv:2408.00714*, 2024. URL https://arxiv.org/abs/2408.00714. 2, 3, 6, 17
- Manolis Savva, Abhishek Kadian, Oleksandr Maksymets, Yili Zhao, Erik Wijmans, Bhavana Jain, Julian Straub, Jia Liu, Vladlen Koltun, Jitendra Malik, et al. Habitat: A platform for embodied ai research. In *Proceedings of the IEEE/CVF international conference on computer vision*, pages 9339–9347, 2019. 2
- Priya Sundaresan, Quan Vuong, Jiayuan Gu, Peng Xu, Ted Xiao, Sean Kirmani, Tianhe Yu, Michael Stark, Ajinkya Jain, Karol Hausman, et al. Rtsketch: Goal-conditioned imitation learning from hand-drawn sketches. In 8th Annual Conference on Robot Learning. 1, 3, 17
- Ashish Vaswani, Noam M. Shazeer, Niki Parmar, Jakob Uszkoreit, Llion Jones, Aidan N. Gomez, Lukasz Kaiser, and Illia Polosukhin. Attention is all you need. In NIPS, 2017. URL https://api.semanticscholar.org/CorpusID:13756489.5
- Chen Wang, Linxi Fan, Jiankai Sun, Ruohan Zhang, Li Fei-Fei, Danfei Xu, Yuke Zhu, and Anima Anandkumar. Mimicplay: Long-horizon imitation learning by watching human play. In *Conference on Robot Learning*, pages 201–221. PMLR, 2023a. 3
- Guanzhi Wang, Yuqi Xie, Yunfan Jiang, Ajay Mandlekar, Chaowei Xiao, Yuke Zhu, Linxi (Jim) Fan, and Anima Anandkumar. Voyager: An open-ended embodied agent with large language models. *ArXiv*, abs/2305.16291, 2023b. URL https://api.semanticscholar.org/CorpusID:258887849. 1
- Zihao Wang, Shaofei Cai, Guanzhou Chen, Anji Liu, Xiaojian Shawn Ma, and Yitao Liang. Describe, explain, plan and select: interactive planning with llms enables open-world multitask agents. *Advances in Neural Information Processing Systems*, 36, 2023c. 1

- Zihao Wang, Shaofei Cai, Anji Liu, Yonggang Jin, Jinbing Hou, Bowei Zhang, Haowei Lin, Zhaofeng He, Zilong Zheng, Yaodong Yang, et al. Jarvis-1: Open-world multi-task agents with memory-augmented multimodal language models. *arXiv preprint arXiv:2311.05997*, 2023d. 1, 3
- Dongshu Xu, Jun Chen, Chao Liang, Zheng Wang, and Ruimin Hu. Cross-view identical part area alignment for person re-identification. In *ICASSP 2019 2019 IEEE International Conference on Acoustics, Speech and Signal Processing (ICASSP)*, pages 2462–2466, 2019. doi: 10.1109/ICASSP.2019.8683137. 3
- Qianfan Zhao, Lu Zhang, Bin He, Hong Qiao, and Zhiyong Liu. Zero-shot object goal visual navigation. In *2023 IEEE International Conference on Robotics and Automation (ICRA)*, pages 2025–2031. IEEE, 2023. 2
- Fangwei Zhong, Kui Wu, Churan Wang, Hao Chen, Hai Ci, Zhoujun Li, and Yizhou Wang. Unrealzoo: Enriching photo-realistic virtual worlds for embodied ai, 2024. URL https://arxiv.org/abs/2412.20977. 2, 14, 16, 18
- Yifan Zhong, Xuchuan Huang, Ruochong Li, Ceyao Zhang, Yitao Liang, Yaodong Yang, and Yuanpei Chen. Dexgraspvla: A vision-language-action framework towards general dexterous grasping, 2025. URL https://arxiv.org/abs/2502.20900. 5

Appendix

Implementation Details and Extended Results

A. Environments

ROCKET-2 is trained in Minecraft (Cai et al., 2024) and evaluated not only within Minecraft but also across a diverse set of **out-of-domain** environments, including Unreal Engine (Zhong et al., 2024), Doom (Kempka et al., 2016), Deep-Mind Lab (Beattie et al., 2016), and several commercial Steam games. Table 4 provides an overview of their observation and action spaces. To enable cross-environment testing, we construct a rule-based mapping from Minecraft's action space to those of the target environments (table 1), without relying on environment-specific fine-tuning or carefully crafted adaptations.

We present qualitative demonstrations in both Minecraft and unseen environments in Figure 10 and Figure 12, where cross-view images with human-provided masks serve as goal specifications. In Minecraft, ROCKET-2 showcases advanced interactive abilities, including defeating the Ender Dragon and constructing long-span bridges—tasks previously unattainable by existing agents. Remarkably, ROCKET-2 also exhibits strong generalization to unfamiliar environments: it performs visually-guided exploration in Unreal Engine, effectively transfers combat behaviors to Doom, and remains robust despite drastic differences in observation styles across games such as Portal and Dark Souls. These results highlight the model's ability to leverage visual cues and make meaningful decisions in a zero-shot setting, underscoring the versatility and generality of cross-view goal alignment.

B. Implementation Details

We present the model architecture, hyperparameters, and optimizer configurations of ROCKET-2 in table 5. During training, each trajectory is divided into segments of length 128 to reduce memory requirements. We initialize the view backbone that is used to encode RGB images with

DINO weights and freeze it for training efficiency. During inference, ROCKET-2 can access up to 128 key-value attention caches of past observations. Most training parameters follow those from prior works such as Baker et al. (2022); Cai et al. (2025a).

Table 5 | Detailed Training Hyperparameters.

Hyperparameter	Value	
Input Image Size	224 × 224	
Hidden Dimension	1024	
View Backbone	ViT-base/16 (DINO-v1)	
Mask Backbone	ViT-tiny/16 (1-channel)	
Spatial Transformer	PyTorch Transformer	
Number of Spatial Blocks	4	
Temporal Transformer	TransformerXL	
Number of Temporal Blocks	4	
Trajectory Chunk size	128	
Optimizer	AdamW	
Learning Rate	0.00004	

C. Training Datasets

We train ROCKET-2 using 1.6 billion frames of human gameplay data collected by OpenAI (Baker et al., 2022). Each frame is annotated with finegrained interaction events, including actions such as mining, crafting, item usage, and combat. This large-scale dataset provides rich behavioral diversity across a wide range of tasks and environmental contexts. Building on the protocol established by ROCKET-1 (Cai et al., 2025a), we further enrich each interaction event with frame-level object masks that identify the involved entities or objects. For each interaction event, we ensure that all associated masks correspond to the same target entity. From these, one masked frame is randomly sampled to serve as the cross-view goal specification for training. This process enables the model to learn to align its current egocentric observation with high-level goals presented from different viewpoints. The interaction types used in training include use, break, approach, craft, and kill entity, following the taxonomy introduced in



Figure 10 | Minecraft Demonstrations. ROCKET-2 showcases a diverse range of skills, including combat with monsters, locating the Ender portal, bridge construction, ore mining, and crafting. Cross-view perspectives with segmented and circled masks are displayed in the top right window. Predicted bounding boxes, visibility, and actions are overlaid on the images, highlighting the agent's robust 3D visual goal understanding and alignment with human-specified targets.

ROCKET-1. These categories cover a broad spectrum of interaction patterns, equipping ROCKET-2 with the ability to generalize across diverse task structures and object affordances.

D. Minecraft Interaction Benchmark

To assess ROCKET-2's ability to accurately interact with target objects under cross-view settings, we adopt the Minecraft Interaction Benchmark introduced in ROCKET-1. This benchmark consists of 12 tasks grouped into six categories: Hunt, Mine, Interact, Navigate, Tool, and Place. Each task requires the agent to identify and interact with specific objects or locations based on visualtemporal prompts. An overview of the benchmark is shown in fig. 11. Compared to prior benchmarks such as Lin et al. (2023), this benchmark places a stronger emphasis on precise spatial interaction—requiring the agent not just to recognize object categories, but to distinguish between multiple instances of the same object type and interact with the correct one at a particular location. This setup significantly raises the bar for visual grounding and spatial understanding, making it a more rigorous testbed for evaluating cross-view interaction capabilities in partially observable 3D environments.

E. Analyzing Failure Cases

We conduct a detailed analysis of failure cases during ROCKET-2's task execution and identify three primary sources of error:

Prediction Drift. When pursuing distant targets over extended sequences, the predicted interaction point gradually drifts away from the actual object. This issue arises because the agent relies heavily on temporal consistency from memory to maintain object identity. However, during training, the model was only exposed to sequences of up to 128 steps. As a result, it struggles to generalize to longer horizons at test time, revealing limitations in its long-range memory modeling.

Distance Perception Error. In cases where the agent's current egocentric view differs significantly from the goal-provided view, we observe that the agent sometimes stops one step short of the target, leading to failed interactions. This suggests a misjudgment of spatial proximity under high viewpoint discrepancy. In particular, updating the goal to reflect the current view of the agent mitigates this problem, indicating that the model encounters larger cross-view gaps during inference than during training, affecting its precision of spatial reasoning.

Action Jitter. When evaluating the original version of ROCKET-2, we notice substantial action

Table 4 | **Overview of Environments.** The **blue line** separates the training environment from the zero-shot evaluation environments. Minecraft is our primary training environment, while others serve for zero-shot generalization assessment.

Environment	Observation Space Details	Action Space Details
Minecraft (Training) (Cai et al., 2024)	 Visual: First-person RGB images (640 × 360). Numerical: Comprehensive player information (e.g., health, food levels); not utilized during training and inference. 	 Discrete actions: attack, back, forward, hotbar, inventory, jump, left, right, sneak, sprint and use. Continuous actions: adjusting pitch and yaw in [-180, 180]. For the output of agent, we take the hierarchical action space (Baker et al. (2022)) of 8,641 discrete button combinations and 121 camera movement bins.
Unreal Engine (Zhong et al., 2024)	 Visual: First-person RGB images as well as goal images (640 × 480). The observation resolution notably differs from that of Minecraft. Goal: The agent must rescue objects and transport them to designated stretchers, requiring exploration of complex 3D environments guided by visual goal cues. 	 Discrete actions: carry, drop, jump, crouch, and open the door. Continuous actions: adjusting angular velocity (turning), linear velocity (moving forward/backward), and viewpoint (masked).
ViZDoom (Kempka et al., 2016)	 Visual: First-person RGB view (e.g., 320 × 240). We use the basic config for demonstration. 	• 3 primary actions are enabled in the basic setting: move left/right, shoot (attack).
DeepMind Lab (Beattie et al., 2016)	 Visual: First-person RGB images (640 × 480). We choose map seekavoid_arena_01, a fruit-gathering environment with navigation scenarios. 	 Discrete actions: move back/forward, fire, jump, crouch, and strafe left/right. Continuous actions: adjusting angular velocity (turning), and viewpoint (masked) in angular per second of game time.
Steam Games (Portal/Dark Souls)	• Visual : First-person RGB view, resized to 640 × 360.	• Same as Minecraft, where output actions are mapped to human keyboard and mouse movements.

jitter—rapid, unstable changes in predicted actions—which often results in failures for tasks requiring fine control, such as block placement. We find that feeding previous actions as input during both training and inference significantly improves action stability, leading to smoother and more reliable behavior.

F. Comparison with ROCKET-1

ROCKET-1 tackles interaction problems in 3D worlds by training a visuomotor policy to identify interaction targets based on semantic segmentations in the visual context. While it resolves traditional goal images' ambiguity and



Figure 11 | Minecraft Interaction Benchmark. The benchmark in ROCKET-1 is designed to test an agent's interaction capabilities with visual goals. The 12 tasks challenge the agent's ability to follow visual cues to interact with objects at precise spatial locations, a key advancement over previous benchmarks. Image credit: Cai et al. (2025a).

generation challenges, it relies on SAM-2 (Ravi et al., 2024) to track goals and segment them during inference, severely limiting real-time performance. Additionally, its frame-by-frame segmentation training fails to build the policy's 3D spatial perception, making it heavily dependent on SAM-2's tracking capabilities. ROCKET-2 is a cross-view segmentation-conditioned policy that. Unlike ROCKET-1, it enables the policy to align the goal across camera views by itself and removes the need for real-time segmentation.

G. Hindsight Trajectory Relabeling

There are two main approaches to collecting labeled trajectory data: (1) providing instructions for contractors to collect trajectories in real-time, ensuring a causal link between actions and labels but incurring high costs and limited scalability; and (2) gathering large amounts of trajectories and generating labels through post-processing, known as hindsight trajectory relabeling. While the first approach (Lynch et al., 2023; Padalkar et al., 2023) produces higher-quality data, its cost constraints have led most research to adopt the second, more scalable one. Andrychowicz et al. (2017) was the first to reinterpret a trajectory's behavior using its final frame, greatly improving data utilization and inspiring subsequent research on goal-conditioned policies. Lifshitz et al. (2023) extended the approach by using the last 16 frames of a trajectory as the more expressive goal. Sundaresan et al. introduced hand-drawn sketches as a goal modality, reducing semantic ambiguity. Gu et al. (2023) converted the robotic end-effector moving sketch to a 2D image as the goal, providing richer procedural details. ROCKET-1 introduced backward trajectory relabeling, which first identifies interaction objects and events, then utilizes object tracking models (Ravi et al., 2024) to generate frame-level segmentations. This data supports training segmentation-conditioned policies. Our paper explores using this dataset to train policies for cross-view goal alignment.

Table 6 | **ROCKETs Inference Pipeline Formulation.** Molmo can locate the target object based on the task prompt. SAM uses the point to generate object mask m_t w.r.t. o_t and supports per-frame tracking.

Model	Inference Pipeline	
R1(3)	$\mathbf{m_1} \leftarrow \text{SAM}(o_1, \text{Molmo}(o_1, \text{prompt}))$ $\pi_{R1}(a_t o_1, \mathbf{m_1}, o_2, o_3, o_4, \mathbf{m_4}, o_5, o_6, o_7, \mathbf{m_7}, \cdots)$	
R1(30)+track	$\mathbf{m}_{1:30} \leftarrow \text{SAM}(o_{1:30}, \text{Molmo}(o_1, \text{prompt}))$ $\pi_{R1}(a_t o_1, \mathbf{m}_1, o_2, \mathbf{m}_2, o_3, \mathbf{m}_3, o_4, \mathbf{m}_4, \cdots)$	
R2(60)	$\mathbf{m_1} \leftarrow \text{SAM}(o_1, \text{Molmo}(o_1, \text{prompt}))$ $\pi_{R2}(a_t o_1, \mathbf{m_1}, o_2, o_3, o_4, \cdots, o_{60}, o_{61}, \mathbf{m_{61}}, \cdots)$	

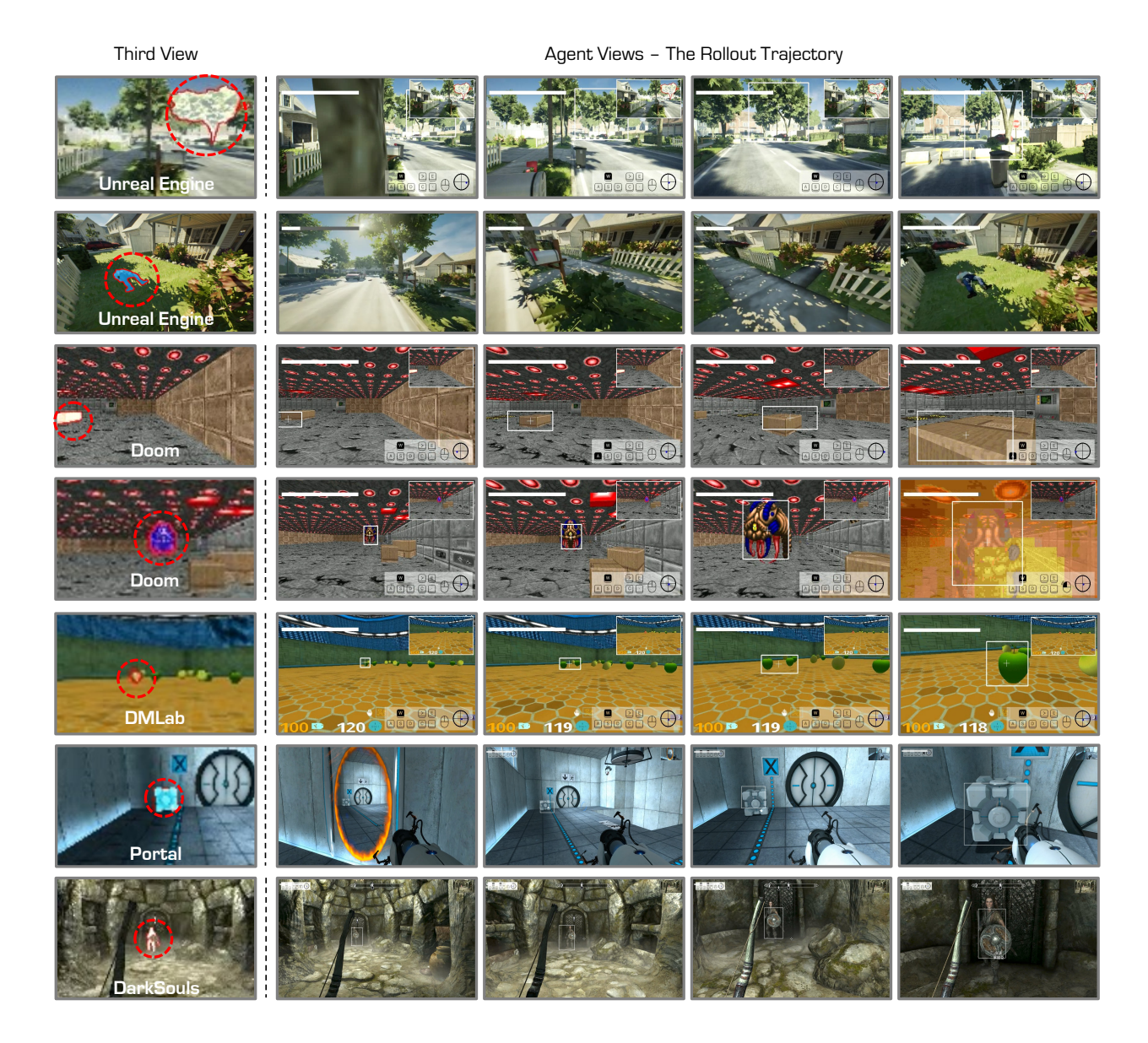


Figure 12 | **Zero-Shot Demonstrations.** We evaluate ROCKET-2 in a variety of previously unseen environments, including Unreal Engine (Zhong et al., 2024), Doom (Kempka et al., 2016), DeepMind Lab (Beattie et al., 2016), Portal, and Dark Souls. Remarkably, ROCKET-2 exhibits strong exploration abilities guided by visual cues in Unreal Engine, successfully transfers certain skills such as attacking in Doom, and maintains robustness to observations that differ significantly from those in Minecraft (Unreal Engine, Portal, and Dark Souls).



Figure 13 | **Training Dataset.** Each row represents a distinct interaction event (such as use, break, or approach) in which all segmentation masks correspond to the same goal. The left column presents sampled cross-view goals and their associated masks for each event, while the right column displays the corresponding frames during that event. This pairing of a cross-view objective with an egocentric action frame constitutes the foundation of our training dataset. In the images, the white point marks the center of the mask, whereas the green point indicates the location predicted by ROCKET-2.